Heat-Dependent Hairpin Melting Drives TRPV1 Opening

Short title: Digital codes in heat-sensing TRPV1

Guangyu Wang*

Department of Physiology and Membrane Biology, University of California School of Medicine, Davis, CA, USA

Department of Drug Research and Development, Institute of Biophysical Medico-chemistry, Reno, NV, USA

* Author to whom correspondence should be addressed; E-mail: gary.wang10@gmail.com

Abstract

Non-covalent interactions in bio-macromolecules are individually weak but collectively important. How they take a concerted action in a complex biochemical reaction network to realize their thermal activity and stability is challenging to study. Now the temperature-dependent structural data of the thermo-gated capsaicin receptor TRPV1 are available to examine a role of temperature-dependent little hairpin sizes and strengths in controlling multiple non-covalent interactions for different gating states and the related temperature sensitivity. The results showed that heat-evoked melting of the biggest little hairpin with a minimal loop size and a weak non-covalent interaction initiates a temperature threshold for channel activation while the smaller little hairpins with strong H-bonds may balance between open and inactivated states for heat efficacy and use-dependent desensitization. Together, both biggest and smaller little hairpins were necessary to regulate the temperature sensitivity. Therefore, this hairpin thermodynamics may be broadly significant for thermal stability and activity of supramolecular architectures. (150 words)

Keywords: desensitization; hairpin thermodynamics; non-covalent interaction; temperature sensitivity; threshold; TRP channel

1. INTRODUCTION

Temperature is important in everyday life. Transient receptor potential (TRP) vanilloid-1 (TRPV1) is well-known as a noxious heat sensor in a primary afferent neuron of the dorsal root and the trigeminal ganglia. Its activation allows sodium or calcium to be permeable to a channel pore. With a temperature activation threshold (~42°C) above a normal human body temperature 37°C and a temperature coefficient Q_{10} (defined as the ratio of equilibrium constants measured 10°C apart) higher than 20, this channel can work as a bio-thermometer to monitor a noxious heat signal above 42°C and to regulate the human body temperature. [1-4] In addition to the physical stimuli, capsaicin can also activate TRPV1, producing hot sensation. As cold can decrease the capsaicin-evoked activity of TRPV1, [5] the same gating pathway seems to be shared by both stimuli. On the other hand, residues sensitive to both physical and chemical stimuli are different in TRPV1, suggesting their different gating pathways. [6-9]

TRPV1 is a homotetramer with each monomer consisting of six transmembrane helices. The first four segments (S1–S4) form a voltage-sensor-like domain (VSLD) while the last two (S5 and S6), together with the intervening loop and the pore helix and the extracellular cap-like pore turret between S5 and S6, are folded as a pore domain. The pore domain is surrounded by the VSLD in a domain-swapped arrangement. The cation conductance pathway centers in the pore domain. A hydrophobic constriction around I697 forms a lower S6 gate while the segment from G643 to D646 (^{643}GMGD^{646}) between S5 and S6 (S5-P-S6) in rat TRPV1 (rTRPV1) acts as a short selectivity filter. The S4–S5 linker, which is a short amphipathic helix and almost parallel to the cytoplasmic membrane, couples the VSLD with the pore domain for channel gating. Thus, the overall structure of the TRPV1 channel resembles that of the voltage-gated ion channel. [10-11] However, TRPV1 has a conserved TRP domain, which runs parallel to the inner leaflet of the membrane by virtue of a sharp bend after S6, not only linking the S6 gate crossing bundle but also interacting with the S4–S5 linker and the pre-S1 domain in favor of allosteric coupling between different gating domains. In addition, the characteristic ankyrin repeats within the cytoplasmic N terminus can tether cytoplasmic N- and C-terminal domains for channel assembly. [11-14] Although the structural basis for the chemical stimuli such as capsaicin has been clear, [15-16] the heat-evoked gating pathway is still unknown for TRPV1 regarding the temperature threshold and sensitivity and desensitization.

Since 2013 a DNA hairpin thermal sensor with a limited poly-A loop size has been created to monitor a change in a biological microenvironment. [17] Its initial hairpin melting curve is similar to the temperature-dependent activation curve of the thermosensitive TRPV channels. Its hairpin melting temperature is also in a threshold range of thermosensitive TRPV channels despite an increase with the smaller or less-flexible loop, the shorter duplexed stem, the more H-bonding pairs at the ends, or the higher ionic strength in an aqueous solution. [1, 6, 18-23] In this regard, it is fitting to ask if the thermosensitive TRPV channels exploit a series of little hairpins with minimal loop sizes and weak noncovalent interactions in the loops to control the temperature thresholds and sensitivity or Q_{10} and gating states. In this computational study, graph theory was used as a novel tool to examine this hypothesis by analyzing the cryo-electron microscopy (cryo-EM) structural data of rTRPV1 with or without phosphatidylinositol (PI)-bound at the capsaicin site around the temperature threshold. This hairpin thermodynamic model generates several melting temperatures (T_m) and structural thermo-sensitivity (Ω_{10}) values which are comparable to the experimental thresholds (Tth) and functional thermo-sensitivity Q_{10} values, respectively. Therefore, these results are consistent with the proposals that the melting temperature of the biggest little hairpin with a minimal loop size and weak noncovalent interactions in the loops may be responsible for the temperature threshold for rTRPV1 activation, and that Q_{10} may be controlled by a change of the total minimal loop sizes of the little hairpins in response to a change of the total non-covalent interactions along the gating pathway from a closed state to an open one within 10°C apart.

2. RESULTS

2.1. The PI-free rTRPV1 Was Closed with the First Biggest Little Hairpin in the VSLD/Pre-S1 interface at 25°C

When capsain competes off the PI lipid at low and high temperatures, this vanilloid compound did not bridge any two amino acid chains in rTRPV1 to cause any little hairpin in the presence of MSP2N2 under the given nanodisc condition. [14] Therefore, the state-dependent cryo-EM structures of PI-free rTRPV1 at different temperatures could be used to examine the role of temperature-dependent little hairpin melting in the gating pathway. At 25°C, several kinds of non-covalent interactions between amino acid side chains along the gating pathway from D388 in the pre-S1 domain to K710 in the TRP domain formed a little hairpin topological loop network in the closed state.

First, H-bonds between different hydrophilic amino acid side chains contributed to the formation of little hairpins. In the pre-S1/VSLD interface, Q423-D427 and D424-R428 were paired for H-bonding. In the VSLD, T449-W549, R455-Y537-K535-Y463, Y495-R499 and Q519-N551 were H-bonded. In the VSLD/S4-S5 linker/TRP/VSLD interfaces, the H-bonding pairs were R491-E709, R557-Q700/T704 and Q560-K694. In the pore domain and its interface with the TRP domain, pairs D576-T685, Y584-T641 and Q691-N695 were also engaged in H-bonds (**Fig. 1A**).

Second, aromatic π interactions also brought about little hairpins. Most of them were located in the VSLD and its interfaces with the pre-S1 domain. For example, E397-Y401-R499, F434-W426/F438/Y555, F438-Y555, Y441-F488/F516/Y555, Y444-F448/F488, M445-W549, Y453-Y454, P456-Y463, V486-F490, Y487-F488/R491, F488-F516, F489-I493/L524, Y495/F517-F496, Y511-L515, F516-N551/Y554, F517-L521, F522-F543, Y530-F531/Y537 and Y554-Y555. In the S4-S5 linker/TRP interface, Q560 formed a CH-π interaction with W697. In the pre-S1/TRP interface, R701 produced a cation-π interaction with W426. In the pore domain, the π-interacting pairs had F580-F584/L678, F589-T593, F591/T670-Y666, Y627/E636-F649, F640-Y666, and F649/Y653/L663-F659 (**Fig. 1A**).

Third, salt bridges included K425-E709 in the pre-S1/TRP interface, R491-E513 and R534-E536 in the VSLD, E648-K656 in the outer pore, and K688-E692 in the S6-TRP interface (**Fig. 1A**).

Taken together, along the gating pathway from D388 to K710, sixty two non-covalent interactions produced the total number of minimal little hairpin sizes as 94 (**Fig. 1A**). Among the multiple little hairpins, although several smaller ones had 0 to 9 minimal residues in the loops, the biggest one was outstanding in the pre-S1/VSLD interface. It had a minimal 21-residue loop from Y401 to Q423, D427, W426, F434, Y555, Y441, F516, F517, F496, Y495, R499 and back to Y401 to control the R499-Y401 π interaction (**Figs. 1B-D**). Because two equivalent H-bonds sealed this biggest little hairpin loop, the predicted melting temperature was about 32°C (**Table 1**).

2.2. PI-free rTRPV1 Opened at 48°C with the Melting of the First Biggest Little Hairpin in the VSLD/pre-S1 Interface

If the first biggest little hairpin with a minimal 21-residue loop in rTRPV1 carries out the single-step melting reaction like DNA hairpins, the calculated melting temperature 32°C should be enough to open it above 32°C (**Table 1**). In agreement with this assumption, when PI-free

rTRPV1 opened at 48°C, the broken Y401-R499 π interaction melted the first biggest little hairpin in the VSLD/pre-S1 interface with several changes along the gating pathway.

Table 1 New parameters of the rTRPV1 bio-thermometer based on the hairpin thermodynamic model

Construct	**Control**	**rTRPV1**			
Lipid environment	MSP2N2	MSP2N2			native
PDB ID	7LPE	7LPB	7LPD	7LPC	7LPC
Lipid PI	free	free	free	bound	bound
Sampling temperature	**48°C**	**25°C**	**48°C**	**48°C**	
Gating state	open	closed	inactivated	closed	closed
# of the biggest little hairpin	2	1	3	4	5
Biggest little loop size (L_{max})	9	21	9	8	13
Equivalent H-bonds in L_{max}	1.0	2.0	2.0	2.0	1.5
Total non-covalent interactions	54	62	66	70	68
Total little hairpin sizes, a.a.	72	94	59	91	93
Calculated melting temperature	46°C	**32°C**	56°C	**58°C**	**43°C**
Measured threshold T_{th}		**<48°C**		**>48°C**	**42°C**
Calculated $\Omega_{10,\,min}$ at E=0.5 kJ/mol		7.48	-4.21	8.86	9.06
Calculated $\Omega_{10,\,mean}$ at E=1.0 kJ/mol		**15.8**	**-9.81**	**21.5**	**21.7**
Calculated $\Omega_{10,\,max}$ at E=3.0 kJ/mol		55.8	-37.5	87.8	86.6
Measured Q_{10}		**16.4**			**22-28.2**
Ref. for T_{th} and Q_{10}		[14]			[1, 14]

In the pre-S1/VSLD/TRP interfaces, the E397-Y401 π interaction and the K425-E709 salt bridge and the Q423-D427 and D424-R428 and R491-D707 H-bonds were disconnected. In the VSLD/S4-S5 linker/TRP interfaces, when the Y554-Y555 π interaction was disrupted, the H-bond moved from R557-T704 to Y554-T704 and the π interaction shifted from Y555-F438 to F559-F438. When the Q560-K694 H bond was disrupted, the R557-E570 H-bond and the W697-R701 CH-π interaction were formed (**Fig. 2A**).

When this conformational change extended to the VSLD, the R491-E513 and R534-E536 salt bridges, the R455-Y537-K535-Y463 and Q519-N551 H-bonds, and the Y441/F516-F488 and F489-I493 and Y530-F531 π interactions were disconnected. In the meanwhile, the new Y495-S510 H-bond and the new R499-D509 salt bridge and the new F448-S481 and Y454-R474 and F489-F490 and V518-F522 π interactions emerged.

When this conformational change extended to the pore domain and its interfaces with the S4-S5 linker and the TRP domain, the E648-K656 and K688-E692 salt bridges and the Q691-N695 H-bond were disrupted. In the meanwhile, the new Y584-Y666 and D601-N628/N652 and T650-N652 and Y653-K656 H-bonds and the E651-K656 salt bridge were born.

By all accounts, the total numbers of all non-covalent interactions and minimal little hairpin sizes along the gating pathway from D388 to K710 dramatically decreased from 62 and 94 to 54 and 72, respectively (**Fig. 2A**). As a result, the structural thermo-sensitivity Ω_{10} was about 15.8, which was similar to the experimental Q_{10} value (16.4). [14] On the other hand, even if one equivalent H-bond sealed the second biggest little hairpin with a minimal 9-residue loop in the VSLD/S4-S5 linker/TRP interfaces to control the stimulatory R557-E570 H-bond, the melting temperature was about 46°C (**Fig. 2C, Table 1**).

2.3. PI-free rTRPV1 Inactivated at 48°C with the Third Biggest Little Hairpin in the Pore Domain

When E570 in the S4-S5 linker further H-bonded with Q700 in the TRP domain at 48°C, the smallest little hairpin with no residue in the loop replaced the second biggest little hairpin to stabilize the R557-E570-Q700 H-bonding network up to the melting temperature 64°C. As a result, the formation of the H410-E692 π interaction and the N695-H410 and Y401-D707 H-bonds in the pre-S1/TRP interface locked the channel in a new state with other changes (**Figs. 3A-C**).

When the F559-F438 π interaction was broken in the S4-S5 linker/VSLD interface, the Y401-E397/R499 π interactions was restored in the pre-S1/VSLD interface. In the VSLD, the F448-S481 and Y454-R474 and F489-F490 and Y495-F496 and F517-F496/L521 π interactions were broken with the R499-D509 salt bridge and the Y495-R499/S510 H-bonds. In the meanwhile, the F438-Y555 and Y441-F488 and P456-Y463 and F489-I493/L524 and Y530-F531 and Y554-Y555 π interactions and the Y463-K535 H-bond and the R534-E536 salt bridge were restored with the new Y444-Q519 and R455-K535 and Y463-Y537 and R491-Q494 H-bonds. Finally, in the outer

pore, the D601-N628/N652 H-bonds were disconnected but the E636-K639 and E651-K656 salt bridges changed to H-bonds and the H-bond moved from T650-N652 to E651-Y653 pairs (**Fig.3A**).

Taken together, although the total number of all non-covalent interactions along the gating pathway from D388 to K710 slightly increased from 54 to 66, the total number of the minimal little hairpin loop sizes significantly decreased from 72 to 59 residues (**Fig. 3A**). In other words, this new state was much more like a closed state but more stable than the open state and thus served as an inactivated state to desensitize the channel activity (**Figs. 1A, 2A, 3A**). In this case, a smaller little hairpin with a minimal 2-residue loop from Y401 to T499, Y495, Q494, R491, Y487, F488, F516, Y554, T704, D707 and back to Y401 may be involved in the inactivation (**Figs. 3A, C, E**). On the other hand, a minimal 9-residue loop from D576 to F580, L678, T685 and back to D576 in the S5-S6 interface became the third biggest little hairpin (**Figs. 3D-E**). When two equivalent H-bonds sealed it, the resultant melting temperature was about 56°C (**Table 1**).

2.4. The Binding of PI to the Vanilloid Site Increased the Temperature Threshold and Sensitivity of rTRPV1

When the resident PI occupies the well-known vanilloid site, rTRPV1 in MSP2N2 cannot open even at 48°C. This closed state of PI-bound rTRPV1 is almost identical between 4°C and 48°C. [14] However, compared to PI-free rTRPV1 at 25°C, there were several differences once the PI lipid linked R409, D509, R557, E570 and Q700 together via H-bonds (**Figs. 4A-B**).

In the pore domain and its interfaces with the S4-S5 linker and the TRP domain, the E648-K656 and K688-E692 salt bridges were disrupted with the formation of the D576-R579 and Y627-E636-K639 and E692-R575 H-bonds and the K571-E570/E692 salt bridges and the D654-F655 π interaction. In the VSLD, the R491-E513 salt bridge, the R455-Y537-K535 and Y495-R499 H-bonds, and the F434-F438 and V486-F490 and F489-I493 and Y495-F496 and Y511-L515 π interactions were disrupted. In the meanwhile, the Y441-Y444 and Y463-Y530 and F489-F490 and Y495-E513 and Y554-R557 π interactions were formed with the Y487-R491 π interaction changing to an H-bond (**Figs. 4A**).

In the VSLD/TRP interface, when the H-bond shifted from R557-T704/Q700 to Y554-T704 pairs, the R491-D707 H-bond was disconnected. In the S4-S5 linker/TRP interface, the Q560-K694 H-bond was also broken but the W697-R701 cation-π interaction appeared. In the pre-S1/TRP interfaces, the new E397-K710 and Y401-D707 and D411-N695 and Q423-R701 H-bonds and the H410-I696 π interaction were added. Finally, in the pre-S1/VSLD interface, the

E397-Y401 π interaction and the Q423-D427 and D424-R428 H-bonds were disrupted with the Y401-R499 CH-π interaction becoming a cation-π interaction (**Figs. 4A**). In this case, the total numbers of the non-covalent interactions and minimal little hairpin loop sizes along the gating pathway were 70 and 93. If the same open state was employed, the structural thermo-sensitivity Ω_{10} would be about 21.5, which was comparable to the Q_{10} value (21.9-28.2) (**Table 1**). [1, 14] However, the tight interaction of rTRPV1 with MSP2N2 allowed the PI pocket to be the fourth biggest little hairpin with a minimum 8-atom loop (**Fig. 4B**). When two equivalent H-bonds sealed this loop, the calculated melting temperature was about 58°C (**Table 1**). That may be why the PI-bound rTRPV1 in MSP2N2 cannot open at 48°C [14]

Once the E697-K710 and Y401-D707 H-bonds were broken in a normal lipid environment, the fifth biggest little hairpin with a minimal 13-residue loop from Y401 to R409, D509, E513, Y495 and R499 and back to Y401 would provide a melting temperature 42°C as a normal threshold to disrupt the Y401-R499 π interaction and the related R409-D509 salt bridge so as to release the nearby PI lipid from the vanilloid site for rTRPV1 opening (**Table 1, Figs. 4A-D**). In that case, the total numbers of the non-covalent interactions and minimal little hairpin loop sizes along the gating pathway would be 68 and 95. If the same open state was employed, the structural thermo-sensitivity Ω_{10} would be about 21.7, which was also comparable to the Q_{10} value (21.9-28.2) (**Table 1**). [1, 14]

3. DISCUSSION

TRPV1 is designed and created as a bio-thermometer in the thermostable system to detect noxious heat and to protect a human or animal body from heat damage. [1-4] To this end, it should meet several protein engineering requirements. First, it should be an integral membrane protein with a relative high physicochemical stability or heat capacity to avoid thermal denaturation. Second, it should be an ion channel that can directly couple a temperature signal to an electronical signal reporter for a readout by a primary afferent sensory neuron. Third, its opening from the closed state within 10°C apart should have a high Q_{10} with a steep response to a small change in a surround predetermined temperature. Fourth, it should have a heat switch with two temperature threshold limits for two gating states, one for activation to sense noxious heat and the other for inactivation to alleviate pain by exploiting use-dependent desensitization upon constant noxious heat stimuli. In the biological and chemical world, a hairpin topological loop structure may be an ideal tool for thermosensitive TRP channels to achieve them.

The DNA hairpin with the limited loop sizes has been designed as a temperature switch, a thermometer and an ionic detector with Q_{10} in the range from 1.8 to 2.7. Its oligonucleotides with complementary nucleotide sequences at the ends form a duplex region as the hairpin stem upon intra-strand hybridization, and its nucleotides in between as the hairpin loop. When a temperature increases above a threshold, the DNA hairpin melts and thus becomes single stranded. Its melting temperature threshold sharply depends on the H-bonded base pairs in the stem, the size and flexibility of the loop and the ionic strength in a solution. Generally, a stable stem or a small and rigid loop or a high salt concentration in the solution allows the DNA hairpin to have a high threshold to sense and to respond to highly specific and small changes in an environmental temperature. When the loop length is decreased from 20 to 10 A's or the H-bonded G-C base-pairs raise from 2 to 4, the melting temperature threshold can be increased more than 20 degrees. Clearly, a short stem favors sharp hairpin melting rather than gradual melting. Since a change in the loop sequence has no significant effect on the melting temperature threshold of the DNA biosensor, [17] once noncovalent interactions create a hairpin topological loop, the hairpin thermodynamics should be comparable between DNA and protein.

Like the DNA hairpin thermal biosensor, at a given physiological salt concentration (150 mM NaCl), when non-covalent interactions made the biggest little hairpin with a minimal loop size along the gating pathway from D388 in the pre-S1 domain to K710 in the TRP domain of rTRPV1, the melting temperature increased with a decreased loop size and an increased number of equivalent H-bonds to seal the loop. In the absence of the PI lipid at the vanilloid site, rTRPV1 had the first biggest little hairpin with a minimal 21-residue loop from Y401 to Q423, D427, W426, F434, Y555, Y441, F516, F517, F496, F495, R499 and back to Y401 in the pre-S1/VSLD interface to control the Y401-R499 π interaction (**Fig. 1**). As two equivalent H-bonds kept this loop, the melting temperature was about 32°C (**Table 1**). Therefore, its melting at 48°C further disrupted the R499-Y401 π interaction in the loop and resulted in the formation of the second biggest little hairpin with a minimal 9-residue loop from R557 to E570, Q560, W697, R701, Q700 and back to R557 (**Fig. 2**). However, the presence of one equivalent H-bond to control the R557-E570 bridge set a melting temperature threshold at about 46°C (**Table 1**). Therefore, at 48°C the formation of the E570-Q700 H-bond further generated the smallest little hairpin with no residue in the loop to increase the melting temperature up to about 64°C via one equivalent H-bond to seal the loop. In this case, the third biggest little hairpin appeared in the S5-S6 interface with a minimal 9-residue

loop from D576 to F580 and L678 and T685 and back to D576 (**Fig.3**). This loop had two equivalent H-bonds so that the melting temperature was about 56°C (**Table 1**). On the other hand, in the absence of the E397-K710 and Y401-D707 H-bonds in a native lipid environment, the fifth biggest little hairpin would have a normal melting temperature 43°C in the presence of 1.5 equivalent H-bonds to seal a minimal 13-residue loop from Y401 to R409, D509, E513, Y495, R499 and back to Y401 (**Table 1, Figs. 4A, 4C, 4D**). Thus, the binding of PI to the vanilloid site may increase the temperature threshold in a normal lipid system. However, once PI-bound rTRPV1 was reconstituted in MSP2N2, the presence of those two H-bonds allowed the PI pocket at the vanilloid site to be the fourth biggest little hairpin with 2 equivalent H-bonds to maintain a minimal 8-atom loop. The resultant melting temperature 58°C could prevent the release of PI from the vanilloid site at 48°C for channel opening (**Table 1, Figs. 4A, 4B, 4D**). Therefore, like a DNA hairpin, a single-step melting reaction of the biggest little hairpin topological loop may be enough to initiate the temperature-dependent threshold in rTRPV1. In accordance with this proposal, in the putative presence of the sixth biggest little hairpin with a minimal 12-residue loop from Y408 to R415, D517, E521, Y503, R507 and back to Y408 (**Fig. 4D**), platypus (*Ornithorhynchus anatinus*) TRPV1 (pTRPV1) decreases an activation threshold by about 3°C. [24]

Despite five biggest little hairpins in rTRPV1, their roles in gating states may be different. The first one was closely coupled to the lower S6 gate via the R499-Y401 π interaction in the VSLD/pre-S1 interface. Therefore, its melting disrupted this non-covalent bridge, allowing PI-free rTRPV1 to open above 32°C (**Table 1, Figs. 1-2**). Although the second biggest little hairpin may favor the open state by uplifting the S4-S5 linker against the S6 gate via the stimulatory R557-E570 H-bond in the VSLD/S4-S5 linker interface, it had an upper melting temperature limit 46°C. Accordingly, when another E570-Q700 H-bond decreased the minimal loop size from 9 residues to zero for a higher melting temperature 64°C to protect the R557-E570 H-bond from the disruption above 46°C, the third biggest little hairpin appeared in the S5-S6 interface increasing the upper melting temperature limit from 46°C to 56°C. In the meanwhile, the presence of the E397-K710 and Y401-D707 H-bonds in the pre-S1/TRP interface may inactivate the channel, alleviating pain upon constant noxious heat stimuli-induced desensitization (**Table 1, Figs. 2-3**). [1, 8, 14] In agreement with this proposal, the absence of a serine residue between S410 and E411 may not allow pTRPV1 to have E404-K718 and Y408-D715 H-bonds in the pre-S1/TRP interface to inactivate pTRPV1 (**Figs. 3E, 4D**). [24] In this regard, the deletion of S404 or the D707A

mutation may stop inactivation of rTRPV1. On the other hand, the cryo-EM structure of pTRPV1 is expected to have closed and open states but not an inactivated state around 40°C in the presence of 150 mM NaCl.

Since the third biggest little hairpin factually had the melting temperature 56°C (**Table 1**), the upper threshold limit for the rTRPV1 bio-thermometer may be 56°C. In the native lipid system, the fifth putative biggest little hairpin with a minimal 13-residue loop in the VSLD/pre-S1 interface may have a normal melting temperature 42°C (**Table 1, Figs. 4C-D**). Like the first one, its melting above 42°C may disrupt the R499-Y401 π interaction in favor of channel opening (**Fig. 5A**). When the salt concentration was lowered down from 150 mM to 130 mM, the threshold may also decrease from 42°C to 37.7°C. [8, 24] On the other hand, when rTRPV1 was reconstituted in MSP2N2, the fourth biggest little hairpin had a minimal 8-atom loop in the PI pocket to prevent PI from release below 58°C. The very high melting temperature in such a lipid system may be beyond the physiological range for the detection of noxious heat unless a vanilloid compound like capsaicin could bind near D509 and R557 to remove the PI lipid (**Table 1, Fig. 4**). [14] Taking all these into account, rTRPV1 may have a bio-thermometer range from 42°C to 56°C to monitor the noxious heat (**Fig.5A**). Further experiments are necessary to examine the role of the Y401-R499 π interaction and the R409-D509 salt bridge in securing the normal temperature threshold 42°C for rTRPV1 opening.

When PI-free rTRPV1 opens at 48°C from a closed state at 25°C, the opening of multiple little hairpins may increase entropy but decrease enthalpy as a result of the decrease in the total non-covalent interactions from 62 to 54 along the gating pathway from D388 to K710 (**Figs 1-2**). [25] Thus, a small decrease in the free energy may be enough for intra-molecular gating rearrangements to activate TRPV1. However, even if several short little hairpin stems were included, such a small decrease may be insufficient to produce a high Q_{10} for noxious heat detection. Therefore, a decrease in the total minimal loop sizes of little hairpins to control the decrease in all the non-covalent interactions and the resultant increase in heat capacity along the gating pathway should be considered. In direct line with this proposal, when the total number of all minimal hairpin sizes dramatically decreased upon the decrease of the total non-covalent interactions, the resultant structural thermo-sensitivity (Ω_{10}) was comparable to the functional thermo-sensitivity (Q_{10}). For PI-free rTRPV1, the calculated Ω_{10} was about 15.8 while the experimental Q_{10} is about 16.4. For PI-bound rTRPV1, the predicted Ω_{10} was about 21.7 while

the experimental Q_{10} is in a range from 21.9 to 28.2. [1, 14] The presence of the PI lipid at the vanilloid site apparently increased both Ω_{10} and Q_{10} values by about 1/3. [14] When the intensity of a non-covalent interaction ranged from the minimal 0.5 kJ/mol to the maximal 3 kJ/mol, the normal Ω_{10} could be in a range from 9.06-86.6 (**Table 1**). Therefore, any measured Q_{10} values may be reasonable in this range.

Taken together, the biggest little hairpins may start the temperature threshold for heat-evoked TRPV1 opening from a closed state while a decrease in the total minimal loop sizes of little hairpins upon a decrease in the total non-covalent interactions along the gating pathway may be responsible the high Q_{10}. In this regard, it is necessary to examine the roles of the second biggest little hairpin and other smaller little hairpins in heat-evoked gating.

The second biggest little hairpin had one equivalent H-bond to seal a minimal 9-residue loop for the open state of rTRPV1 (**Figs. 2, 5A**). As the mutation R557E/A/L or E570L/A can disrupt the stimulatory R557-E570 H-bond, it is reasonable that the R557E or E570L mutant leads to a complete loss of function, or mutants R557A/L and E570A have low heat sensitivity, or E570A increases the threshold from 41.5°C to 44.3°C. [26, 27]

The first smaller little hairpin had no residue in the loop from Y441 and through F516 and Y554 and Y555 and back to Y441. It was shared by both closed and open states (**Figs 1-2, 5B**), and the related aromatic residues were highly conserved in thermosensitive TRPV1-4 but not in non-thermosensitive TRPV5-6. [28] The tight π interactions may allow it to serve as a relatively stationary anchor against which the S4–S5 linker can uplift in favor of TRPV1 opening. In support of this notion, the Y441S, Y444S, Y554A or Y555S mutation leaves the channel not functional. [26, 29]

The second smaller little hairpin had a minimal 6-residue loop from D576 to K579 and F580 and L678 and T685 via the D576-T685 and D576-R579 H-bonds and the F580-L678 CH-π interaction (**Fig. 4A**). The D576-R579 H-bond was disrupted in the open state (**Fig. 2**). It has been reported that the mutant R579E is not functional and the D576N/R or R579A mutant is less sensitive to heat than wild type rTRPV1. [26] Since the residues for this smaller little hairpin are conserved in TRPV1-6, it may serve as a key common anchor in the pore domain. [28]

The third smaller little hairpin had no residue in the loop from Y584 to T641 and F640 and Y666 and back to Y584 (**Fig. 5B**). The residues for this smallest hairpin were also highly conserved in TRPV1-4 but not in TRPV5-6. [28] In agreement with its importance, the Y666A

mutation is not functional while the F640L or T641S mutation decreases the temperature threshold to allow them to be constitutively active at room temperature. [30-31]

The fourth smaller little hairpin had no residue in the loop from Y627 to N628, D601, N652, T650, F649 and back to Y627 to stabilize the open state (**Figs. 2A, 5B**). It has been reported that the N628K or N652T or Y653T or combined mutation increases the temperature threshold, and the triple mutant N628K/N652T/Y653T has the longer opening durations [7] Furthermore, the N628L mutation greatly decreases the heat sensitivity (Q_{10}~2.6) but the N628D mutation has the opposite effect (Q_{10}~86), [14] possibly by mediating the heat stablity of this smaller little hairpin. On the other hand, the turret deletion or replacement with glycine between G603 and N626 in mouse TRPV1 (mTRPV1) decreases the temperature threshold to a different extent, [8] possibly by weakening the corresponding R500-Y402 π interaction in the VSLD/pre-S1 interface or generating another new biggest little hairpin with a minimal size larger than 13 residues in the loop along the gating pathway from D389 to K711. Notably, although the deletion of the turret (Δ604-626) still allows the TRPV1 mutant construct to be activated by heat, the binding of external double-knot toxin or vanilla-toxin (DkTX) to the outer pore prevents heat activation, [9, 15] possibly by affecting the smallest little hairpins in the outer pore (**Fig.5**).

The fifth smaller little hairpin had no residue in the loop linking W426 on pre-S1, F434 and F438 on S1, F559 and Q560 in the S4-S5 linker, and W697 and R701 in the TRP domain together. This little hairpin topological loop may play a critical role in stabilizing the open state (**Figs. 2, 5B**). The sixth smaller hairpin had no residue in the loop from Y444 to M445, W549, T449, F448 and back to Y544. It was highly conserved in all the gating states and thus may serve as a static anchor (**Figs. 1-5**). Further experiments are necessary to test these possibilities.

4. CLOSING REMARK

The little hairpin topological loop structures can be used to design a thermosensitive bio-thermometer with a high Q_{10} value. In addition to the ionic strength in the physiological range, the little hairpin size and the number and the intensity of the hairpin-forming non-covalent interactions between amino acid side chains in a complex biochemical reaction network can be used to tune the little hairpin strength for different melting temperature thresholds to detect distinct small environmental temperature changes. These non-covalent interactions include salt bridges, aromatic side chain π interactions and H-bonds. Both the biggest and smaller little hairpins are necessary to control the temperature threshold and the thermal efficacy. Their opening and closure

should be reversible and fast enough to have a very large effect on channel gating, which can be easily coupled to an electrical readout in the primary afferent sensor neuron. In this regard, this study may provide a broad structural basis for thermosensitive TRP channels to work as a bio-thermometer. On the other hand, although a given non-covalent interaction's spatial and geometric requirements has been well-understood, it is still hardly predictable in a complex temperature-dependent biochemical reaction network. In this regard, this hairpin thermodynamic model, once examined by the temperature-dependent structural data of TRPV1, may provide more creative metrics for identifying causal structure–activity/selectivity relationships in a supramolecular architecture at a variety of ambient temperatures.

5. MATERIALS AND METHODS

In this computational study, the little hairpin topological structural aspects of rTRPV1 channels below and above the temperature threshold were investigated and analyzed with graph theory as the bio-thermometer basis for noxious heat detection. The *in silico* protomer models were based on the cryo-EM structural data of closed rTRPV1 in MSP2N2 with PI-bound at 4°C (PDB ID, 7LP9, model resolution= 2.63 Å) and 48°C (PDB ID, 7LPC, model resolution= 3.07 Å), capsaicin-bound at 25°C (PDB ID, 7LPB, model resolution= 3.54 Å) and 48°C (PDB ID, 7LPD, model resolution= 3.55 Å), and open rTRPV1 with capsaicin-bound at 48°C (PDB ID, 7LPE, model resolution= 3.72 Å), [14] UCSF Chimera was used to assess non-covalent interactions in TRPV1. All the stereo- or regioselective diagonal and lateral non-covalent interactions such as salt-bridges and lone pair/CH/cation-π interactions and H-bonds between amino acid side chains along the gating pathway from D388 in the pre-S1 domain to K710 in the TRP domain of rTRPV1 were included to test their potential roles in forming the little hairpins with minimal loop sizes, controlling the temperature threshold and stablizing the heat afficacy for the higher temperature coefficient Q_{10}.

The standard definition of noncovalent interactions was employed. A hydrogen bond was considered present when the angle donor-hydrogen-acceptor was within the cut-off of 60°, and when the hydrogen-acceptor distance is within 2.5 Å and the maximal distance is 3.9 Å between a donor and an acceptor. A salt bridge was considered to be formed if the distance between any of the oxygen atoms of acidic residues and the nitrogen atoms of basic residues were within the cut-off distance of 3.2-4 Å in at least one frame. When the geometry was acceptable, a salt bridge was also counted as a hydrogen bonding pair. The face-to-face π-π stacking of two aromatic rings was

considered effective once the separation between the π-π planes was ~3.35-4.4 Å, which is close to at least twice the estimated van der Waals radius of carbon (1.7Å). The edge-to-face π-π interaction of two aromatic rings was considered attractive when the cut-off distance between two aromatic centers was within 4-6.5 Å. Significant cation-π interactions occurred within a distance of 6.0 Å between a cation and an aromatic center. The short effective CH/π distances was 2.65-3.01 Å between aromatic groups, and 2.75-2.89 Å between CH_3 and an aromatic ring. The lone pair-π interaction distance between a lone electron pair and an aromatic ring was within 3-3.7 Å.

The minimal loop sizes in the little hairpin to control the non-covalent interactions were calculated using graph theory. The primary amino acid sequence line from D388 to K710 was marked in black. An amino acid side chain or an atom of a bound lipid involving a non-covalent interaction along the gating pathway of rTRPV1 was represented as a vertex (v) or a node and marked with an arrow in different colors. The same kind of non-covalent interactions was marked in the same color. Any link between two vertices was represented an edge in a biochemical reaction network. A hairpin topologicval loop was formed between two vertices *i* and *j* (v_i and v_j), if and only if there was a path from v_i to v_j and a return path from v_j to v_i. The loop path length (L) was definded as the total number of residues in protein or atoms in the bound lipid that do not participate in any non-covalent interctions in a little hairpin loop. For a given biochemical reaction network, the minimal loop path length (L_{min}) between v_i and v_j was the sum of the shortest return path distance from node *j* to i because the direct shortest path distance from node *i* to *j* was zero when a non-covalent interaction existed between them. The simplest way to find the minimal loop was to identify the shortest return path between two vertices *i* and *j* (v_i and v_j) by using the Floyd-Warshall algorithm. [32] For example, in the biochemical reaction network of Fig.1A, a direct path length from E636 and F649 was zero because there was a π interaction between them. However, there was another shortest return path from F649 to F659, L663, Y666, F640 and back to E636 via three π interacting bridges and two residues between L663 and Y666 and three residues between F640 and E636. Therefore, the minimal little hairpin loop path length was 5. After each non-covalent interaction was tracked by a minimal loop length and marked in black, the total number of all noncovalent interactions and minimal hairpin loop lengths along the gating pathway were shown in black and blue circles, respectively.

The temperature threshold was calculated from the melting temperature T_m of the biggest little hairpin along the gating pathway using the following equation: [17]

$$T_m\ (°C) = 34 + (n-2)\times 10 + (20-L_{max})\times 2$$

where, n is the total number of the non-covalent interactions equivalent to H-bonds in the biggest little hairpin, and L_{max} is the loop length of the biggest little hairpin.

If a thermosensitive ion channel changes from a closed state to an open state within a temperature range ΔT, $\Omega_{\Delta T}$ was defined to evaluate the structural thermo-sensitivity of a single ion channel as calculated using the following equation:

$$\Omega_{\Delta T} = [(L_c - L_o)E/2]^{(Nc/No)}$$

where, L_o and L_c are the total numbers of all the minimal lengths of little hairpins along the gating pathway in the open and closed states, respectively; N_c and N_o are the total numbers of all the non-covalent interactions along the gating pathway in the closed and open states, respectively; E is the energy intensity of a non-covalent interaction in a range of 0.5-3 kJ/mol. Usually, E=1 kJ/mol.

When ΔT=10°C, Ω_{10} could be comparable to the functional thermo-sensitivity (Q_{10}) of a single ion channel. Q_{10} was calculated using the following equation:

$$Q_{10} = (R2/R1)^{10/(T2-T1)}$$

where, R1 and R2 are rates of a reaction at two different temperatures T1 and T2 in Celsius degrees or kelvin, respectively.

Conventions and Abbreviations: cryo-EM, cryo-electron microscopy; DkTx, double-knot toxin or vanillotoxin; PI, phosphatidylinositol; TRP, transient receptor potential; TRPV1, TRP vanilloid-1; TRPVi (i=1; 2, 3, 4, 5, 6); hTRPV1, human TRPV1; mTRPV1, mouse TRPV1; pTRPV1, platypus TRPV1; rTRPV1, rat TRPV1; VSLD, voltage-sensor-like domain

Acknowledgements

The author's own studies cited in this article were supported by NIDDK Grant (DK45880 to D.C.D.) and Cystic Fibrosis Foundation grant (DAWSON0210) and NIDDK grant (2R56DK056796-10) and American Heart Association (AHA) Grant (10SDG4120011 to GW).

Conflict of Interest: The author declares no conflict of interest.

Data Availability Section: This study includes no data deposited in external repositories

References

1. Caterina MJ, Schumacher MA, Tominaga M, Rosen TA, Levine JD, Julius D. The capsaicin receptor: a heat-activated ion channel in the pain pathway. *Nature* **1997**, 389, 816.
2. Davis JB, Gray J, Gunthorpe MJ, Hatcher JP, Davey PT, Overend P, Harries MH, Latcham J, Clapham C, Atkinson K, Hughes SA, Rance K, Grau E, Harper AJ, Pugh PL, Rogers DC, Bingham S, Randall A, Sheardown SA. Vanilloid receptor-1 is essential for inflammatory thermal hyperalgesia. *Nature* **2000**, 405,183.
3. Gavva NR, Treanor JJS, Garami A, Fang L, Surapaneni S, Akrami A, Alvarez F, Bak A, Darling M, Gore A, Jang GR, Kesslak JP, Ni L, Norman MH, Palluconi G, Rose MJ, Salfi M, Tan E, Romanovsky AA, Banfield C, Davar G. Pharmacological blockade of the vanilloid receptor TRPV1 elicits marked hyperthermia in humans. *Pain* **2008**, 136, 202.
4. Vandewauw I, De Clercq K, Mulier M, Held K, Pinto S, Ranst NV, Segal A, Voet T, Vennekens R, Zimmermann K, Vriens J, Voets T. A TRP channel trio mediates acute noxious heat sensing. *Nature* **2018**, 555, 662.
5. Chung MK, Wang S. Cold suppresses agonist-induced activation of TRPV1. *J Dent Res* **2011**, 90, 1098.
6. Jordt SE, Julius D. Molecular basis for species-specific sensitivity to “hot” chili peppers. *Cell* **2002**, 108, 421.
7. Grandl J, Kim SE, Uzzell V, Bursulaya B, Petrus M, Bandell M, Patapoutian A. Temperature-induced opening of TRPV1 ion channel is stabilized by the pore domain. *Nat Neurosci.* **2010**, 13, 708.
8. Cui Y, Yang F, Cao X, Yarovoy VY, Wang KW, Zheng J. Selective disruption of high sensitivity heat activation but not capsaicin activation of TRPV1 channels by pore turret mutations. *J. Gen. Physiol.* **2012**, 139, 273.
9. Jara-Oseguera A, Bae C, Swartz KJ. An external sodium ion binding site controls allosteric gating in TRPV1 channels. *Elife* **2016**, 5.
10. Long SB, Campbell EB, Mackinnon R. Crystal structure of a mammalian voltage-dependent Shaker family K^+ channel. *Science* **2005**, 309, 897.

11. Liao M, Cao E, Julius D, Cheng Y. Structure of the TRPV1 ion channel determined by electron cryo-microscopy. *Nature* **2013**, 504,107.
12. Cao E, Liao M, Cheng Y, Julius D. TRPV1 structures in distinct conformations reveal activation mechanisms. *Nature* **2003**, 504, 113.
13. Nadezhdin KD, Neuberger A, Nikolaev YA, Murphy LA, Gracheva EO, Bagriantsev SN, Sobolevsky AI. Extracellular cap domain is an essential component of the TRPV1 gating mechanism. *Nat Commun.* **2021**, 12, 2154.
14. Kwon DH, Zhang F, Suo Y, Bouvette J, Borgnia MJ, Lee SY. Heat-dependent opening of TRPV1 in the presence of capsaicin. *Nat Struct Mol Biol*. **2021**, 28, 554.
15. Gao Y, Cao E, Julius D, Cheng Y. TRPV1 structures in nanodiscs reveal mechanisms of ligand and lipid action. *Nature* **2016**, 534, 347.
16. Wang G. Lipid-dependent sequential allosteric activation of heat-sensing TRPV1 channels by anchor-stereoselective "hot" vanilloid compounds and analogs. *Biochem. Biophys. Rep*. **2000**, 28, 101109.
17. Jonstrup AT, Fredsøe J, Andersen AH. DNA Hairpins as Temperature Switches, Thermometers and Ionic Detectors. *Sensors* **2013**, 13, 5937.
18. .Caterina MJ, Rosen TA, Tominaga M, Brake AJ, Julius D. A capsaicin-receptor homologue with a high threshold for noxious heat. *Nature* **1999**, 398,436.
19. Caterina MJ, Leffler A, Malmberg AB, Martin WJ, Trafton J, Petersen-Zeitz KR, Koltzenburg M, Basbaum AI, Julius D. Impaired nociception and pain sensation in mice lacking the capsaicin receptor. *Science* **2000**, 288, 306.
20. Peier AM, Reeve AJ, Andersson DA, Moqrich A, Earley TJ, Hergarden AC, Story GM, Colley S, Hogenesch JB, McIntyre P, Bevan S, Patapoutian A. A heat-sensitive TRP channel expressed in keratinocytes. *Science*. **2002,** 296, 2046.
21. Smith GD, Gunthorpe MJ, Kelsell RE, Hayes PD, Reilly P, Facer P, Wright JE, Jerman JC, Walhin J-P, Ooi L, Egerton J, Charles KJ, Smart D, Randall AD, Anand P, Davis JB. TRPV3 is a temperature-sensitive vanilloid receptor-like protein. *Nature* **2002**, 418, 186.
22. Xu H, Ramsey IS, Kotecha SA, Moran MM, Chong JA, Lawson D, Ge P, Lilly J, Silos-Santiago I, Xie Y, DiStefano PS, Curtis R, Clapham DE. TRPV3 is a calcium-permeable temperature-sensitive cation channel. *Nature* **2002**, 418, 181.

23. Chung MK, Lee H, Caterina MJ. Warm temperatures activate TRPV4 in mouse 308 keratinocytes. *J. Biol. Chem*. **2003**, 278, 32037.
24. Luo L, Wang Y, Li B, Xu L, Kamau PM, Zheng J, Yang F, Yang S, Lai R. Molecular basis for heat desensitization of TRPV1 ion channels. *Nat Commun.* **2019,** 10, 2134. Correction in: *Nat Commun*. **2020,** 11, 1798.
25. Kiehna SE, Waters ML. Sequence dependence of β-hairpin structure: Comparison of a salt bridge and an aromatic interaction. *Protein Science* **2003**, 12, 2657.
26. Boukalova S, Marsakova L, Teisinger J, Vlachova V. Conserved residues within the putative S4–S5 region serve distinct functions among thermosensitive vanilloid transient receptor potential (TRPV) channels. *J. Biol. Chem*. **2010**, 285, 41455.
27. .Kim M, Sisco NJ, Hilton JK, Montano CM, Castro MA, Cherry BR, Levitus M, Horn WDV. Evidence that the TRPV1 S1-S4 membrane domain contributes to thermosensing. *Nat Commun.* **2020**, 11, 4169.
28. .Nadezhdin KD, Neuberger A, Trofimov YA, Krylov NA, Sinica V, Kupko N, Vlachova V, Zakharian E, Efremov RG, Sobo-levsky AI. Structural mechanism of heat-induced opening of a temperature-sensitive TRP channel. *Nat. Struct. Mol. Biol.* **2021,** 28, 564–572.
29. .Boukalova S, Teisinger J, & Vlachova V. Protons stabilize the closed conformation of gain-of-function mutants of the TRPV1 channel. *Biochim. Biophys. Acta*. **2013,** 1833,520.
30. .Susankova K, Ettrich R, Vyklicky L,. Teisinger J,. Vlachova V. Contribution of the Putative Inner-Pore Region to the Gating of the Transient Receptor Potential Vanilloid Subtype1 Channel (TRPV1). *J. Neurosci.* **2007,** 27, 7578.
31. Myers BR, Bohlen CJ, Julius D. A yeast genetic screen reveals a critical role for the pore helix domain in TRP channel gating. *Neuron* **2008**, 58, 362.
32. Floyd RW.) Algorithm-97 - Shortest Path. *Commun Acm* **1962**, 5, 345–345.

Figure legends

Figure 1. **The little hairpin topological structural network along the gating pathway of PI-free rTRPV1 in the closed state at 25°C. A,** The little hairpin topological loop map. The cryo-EM structure of closed rTRPV1 with capsaicin bound at 25°C (PDB ID, 7LPB) was used for the model.[14] The pore domain, the S4-S5 linker, the TRP domain, the VSLD and the pre-S1 domain are indicated in black. Salt bridges, π interactions, and H-bonds between pairing amino acid side chains along the gating pathway from D388 to K710 are marked in purple, green, and orange, respectively. The minimal loop sizes in the little hairpins required to control the relevant non-covalent interactions are labeled in black. The total numbers of all minimal hairpin loop sizes and non-covalent interactions along the gating pathway are shown in the blue and black circles, respectively. **B,** The location of the first biggest little hairpin in the pre-S1/VSLD interface. **C,** The structure of the 1st biggest little hairpin with a minimal 21-residue loop in the VSLD/pre-S1 interface to control the Y401-R499 π interaction. **D,** The sequences of the 1st biggest little hairpin to control the R499-Y401 π interaction in the blue box.

Figure 2. **The little hairpin topological structural network along the gating pathway of PI-free rTRPV1 in the open state at 48°C. A,** The little hairpin topological loop map. The cryo-EM structure of open rTRPV1 with capsaicin bound at 48°C (PDB ID, 7LPE) was used for the model.[14] The pore domain, the S4-S5 linker, the TRP domain, the VSLD and the pre-S1 domain are indicated in black. Salt bridges, π interactions, and H-bonds between pairing amino acid side chains along the gating pathway from D388 to K710 are marked in purple, green, and orange, respectively. The minimal loop sizes in the little hairpins required to control the relevant non-covalent interactions are labeled in black. The total numbers of all minimal hairpin loop sizes and non-covalent interactions along the gating pathway are shown in the blue and black circles, respectively. **B,** The structure of the little hairpin with no residue in the loop in the VSLD to replace the R499-Y401 π interaction with the R499-D509 salt bridge. **C,** The structure of the 2nd biggest little hairpin with a minimal 9-residue loop in the VSLD/S4-S5 linker/TRP interfaces to control the stimulatory R557-E570 H-bonded bridge. **D,** The sequences of two little hairpins with minimal 0- and 9-residue loops to control the R499-D509 salt bridge and the R557-E570 bridge in the blue boxes, respectively.

Figure 3. **The little hairpin topological structural network along the gating pathway of PI-free rTRPV1 in the desensitized state at 48°C. A,** The little hairpin topological loop map. The cryo-EM structure of inactivated rTRPV1 with capsaicin bound at 48°C (PDB ID, 7LPD) was used for the model.[14] The pore domain, the S4-S5 linker, the TRP domain, the VSLD and the pre-S1 domain are indicated in black. Salt bridges, π interactions, and H-bonds between pairing amino acid side chains along the gating pathway from D388 to K710 are marked in purple, green, and orange, respectively. The minimal loop sizes in the little hairpins required to control the relevant non-covalent interactions are labeled in black. The total numbers of all minimal hairpin loop sizes and non-covalent interactions along the gating pathway are shown in the blue and black circles, respectively. **B,** The structure of the little hairpin with no residue in the loop in the VSLD/S4-S5 linker/TRP/VSLD interfaces to govern the R557-E570-Q700 H-bond network. **C,** The structure of the putative little hairpin in the VSLD/pre-S1/TRP/VSLD interfaces to control the Y401-D707 H-bond for inactivation and desensitization. **D,** The structure of the 3rd biggest little hairpin with a minimal 9-residue loop in the S5-S6 interface to control the D576-T685 H-bond. **E,** The sequences of three little hairpins with minimal 0-, 2-, and 9-residue loops to control the R557-E570-Q700 H-bond network, the Y401-D707 H-bond, and the D576-T685 H-bond in the blue rectangles, respectively.

Figure 4. **The little hairpin topological structural network along the gating pathway of PI-bound rTRPV1 in the closed state at 48°C. A,** The little hairpin topological loop map. The cryo-EM structure of closed rTRPV1 with PI bound at 48°C (PDB ID, 7LPC) was used for the model.[14] The pore domain, the S4-S5 linker, the TRP domain, the VSLD and the pre-S1 domain are indicated in black. Salt bridges, π interactions, and H-bonds between pairing amino acid side chains along the gating pathway from D388 to K710 are marked in purple, green, and orange, respectively. The minimal loop sizes in the little hairpins required to control the relevant non-covalent interactions are labeled in black. The total numbers of all minimal hairpin loop sizes and non-covalent interactions along the gating pathway are shown in the blue and black circles, respectively. The dashed lines are absent in the native lipid system. The putative little hairpin loop sizes in the native lipid system are labled in grey. **B,** The structure of the 4th biggest little hairpin with a minimal 8-atom loop for the PI pocket. **C,** The structure of the 5th biggest little hairpin

with a minimal 13-residue loop in the VSLD/pre-S1 interface to control the Y401-R499 cation-π interaction near PI. **D,** The sequences of the 4th, 5th, and 6th biggest little hairpins with minimal 8-, 13-, and 12-residue loops to control the PI pocket in rTRPV1, the Y401-R499 π interaction in rTRPV1, and the Y408-R507 π interaction in pTRPV1, respectively. The controlled bridges are marked in the blue rectangles.

Figure 5. The tentative model for TRPV1 opening and desensitization upon the heat-evoked melting of the biggest little hairpin. A. The cryo-EM structures of rTRPV1 in the closed and open and desensitized states (PDB ID: 7LPC, 7LPE, 7LPD, respectively) were used for the model. [14] In the presence of PI at the capsaicin site, rTRPV1 is closed below the threshold 42°C and has the biggest little hairpin with one and half equivalent H-bonds sealing a minimal 13-residue loop (red) to control the VSLD/pre-S1 interface. When the temperature increases above the threshold 42^0C, rTRPV1 is open upon the melting of the fifth biggest little hairpin in the VSLD/pre-S1 interface. In the meantime, the second biggest little hairpin with one equivalent H-bond sealing a minimal 9-residue loop (red) is formed in the VSLD/S4-S5 linker/TRP/VSLD interfaces for the open state. However, in the desensitized state, rTRPV1 further inactivates in the presence of the third biggest little hairpin with two equivalent H-bonds sealing a minimal 9-residue loop in the S5-S6 interface in the temperature range from 42°C to 56°C. **B,** The proposed smallest little hairpins for TRPV1 gating. The minimal loop sizes in little hairpins are shown in the red circles.

Figures

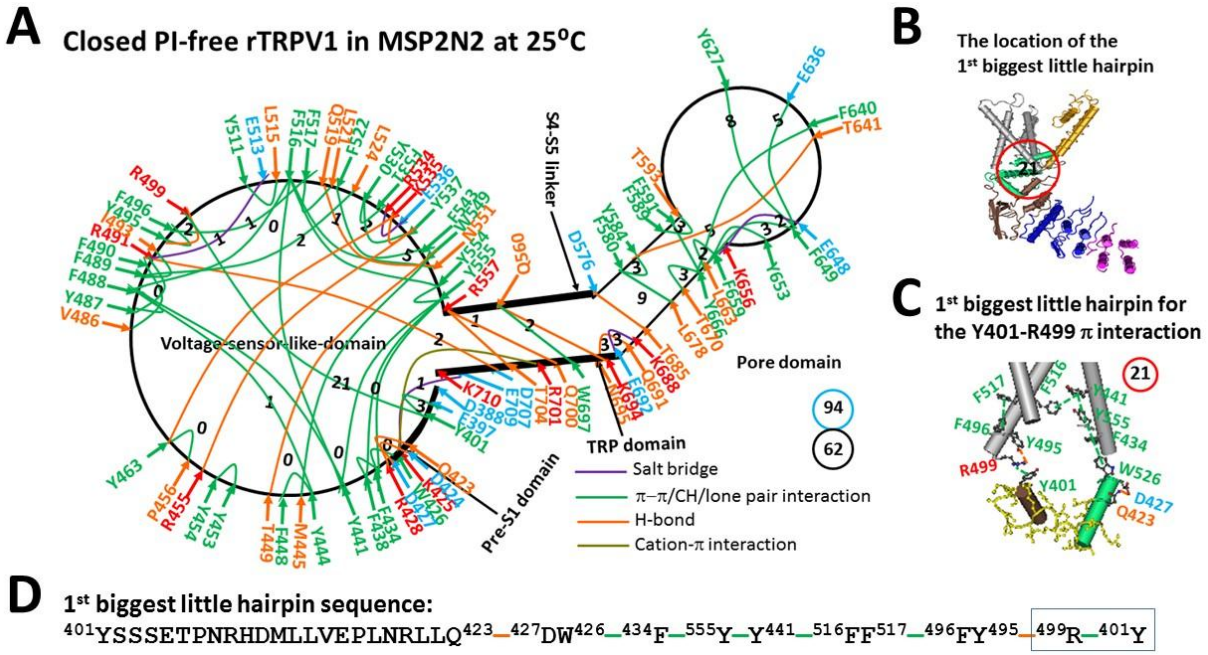

Figure 1

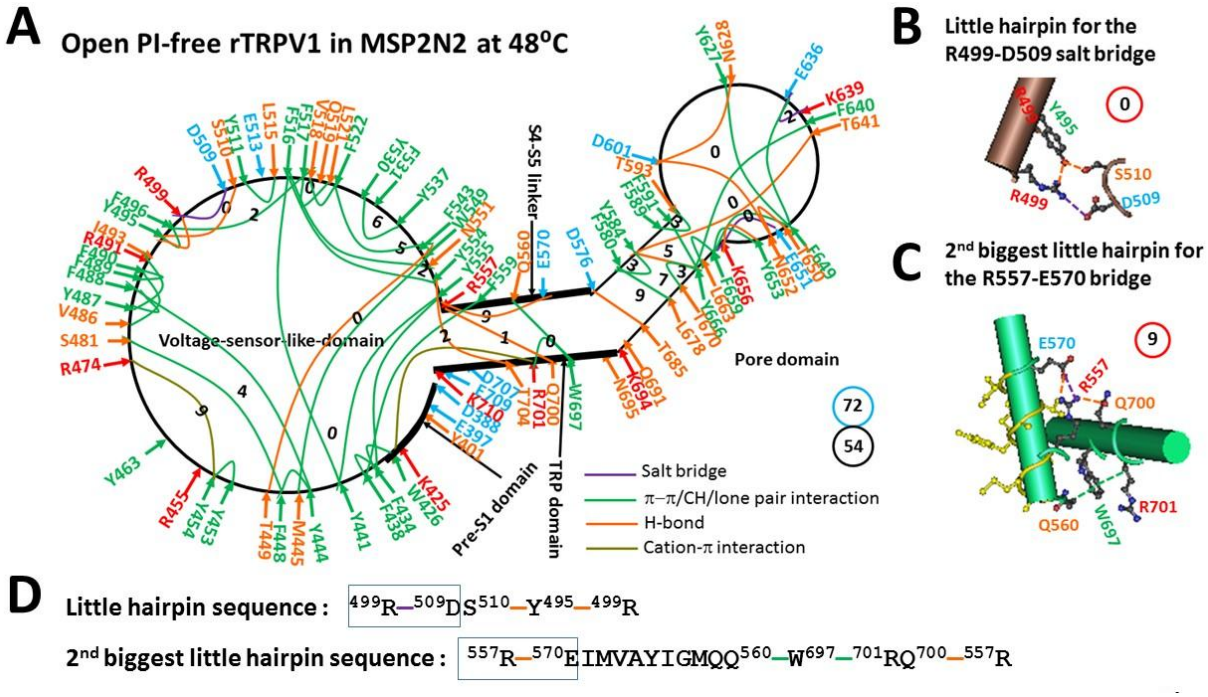

Figure 2

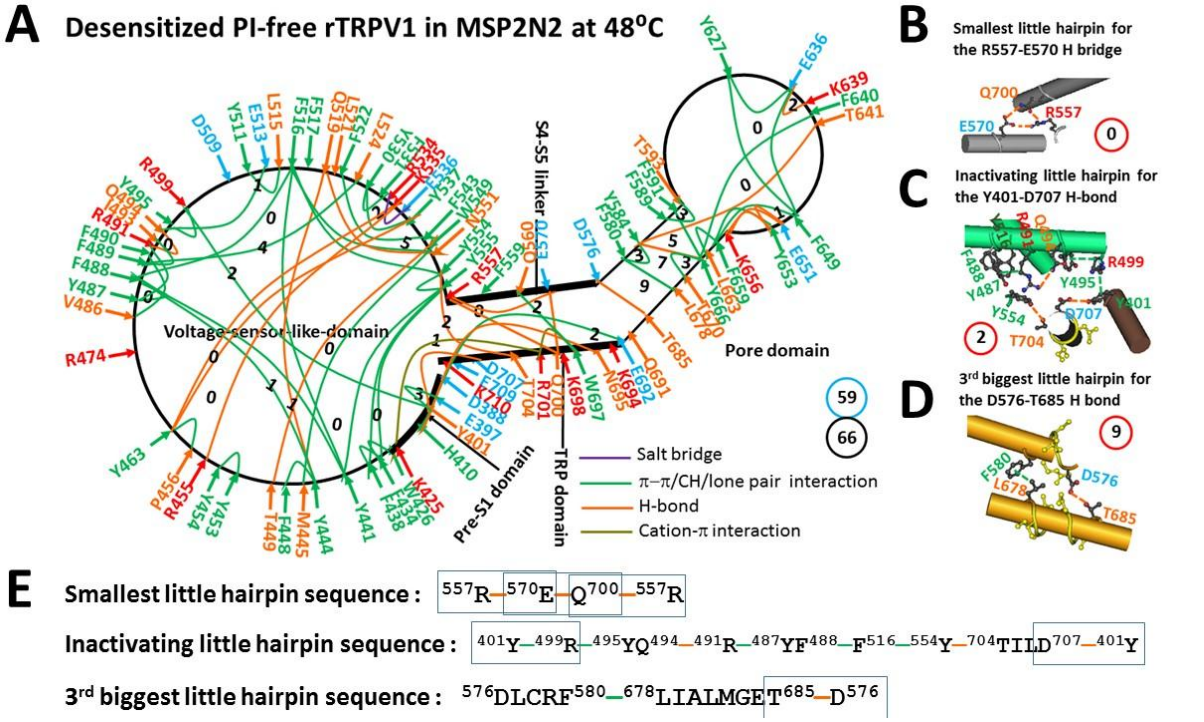

E **Smallest little hairpin sequence :** ^{557}R–^{570}E–Q^{700}–^{557}R

Inactivating little hairpin sequence : ^{401}Y–^{499}R–^{495}YQ^{494}–^{491}R–^{487}YF^{488}–F^{516}–^{554}Y–^{704}TILD^{707}–^{401}Y

3rd biggest little hairpin sequence : ^{576}DLCRF^{580}–^{678}LIALMGET^{685}–D^{576}

Figure 3

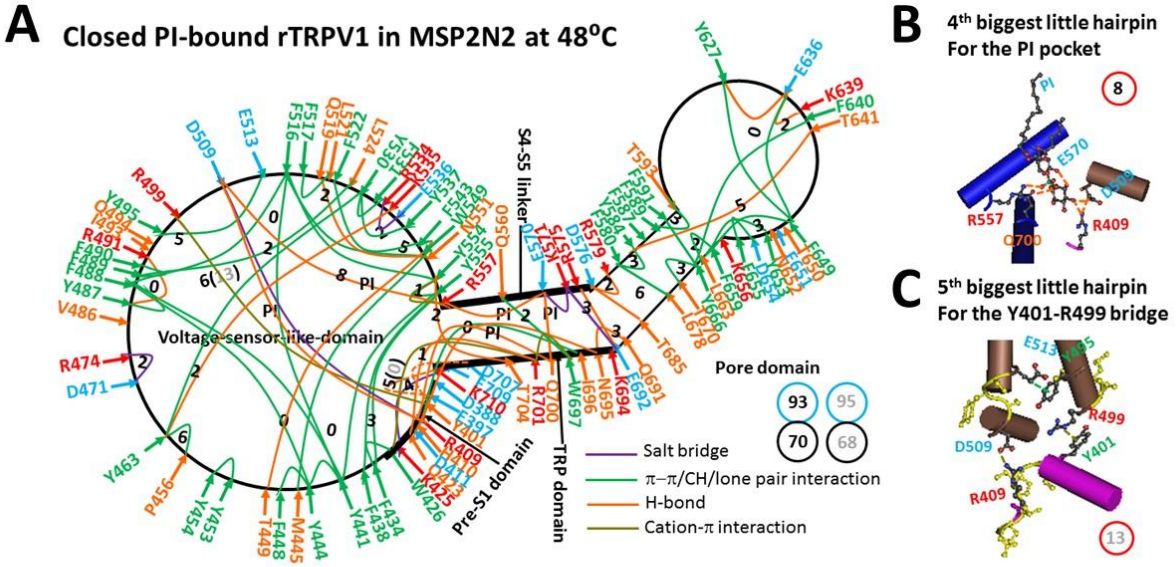

D **rTRPV1 4th biggest little hairpin sequence :** PI–^{557}R–PI–^{700}Q–PI–^{409}R–PI–^{509}D–PI–^{570}E–PI

rTRPV1 5th biggest little hairpin sequence : ^{401}YSSSETPNR^{409}–^{509}DSYSE^{513}–^{495}YFLQR^{499}–^{401}Y

pTRPV1 6th biggest little hairpin sequence : ^{408}YSS ETPNR^{415}–^{517}DSYSE^{521}–^{503}YFLQR^{507}–^{408}Y

Figure 4

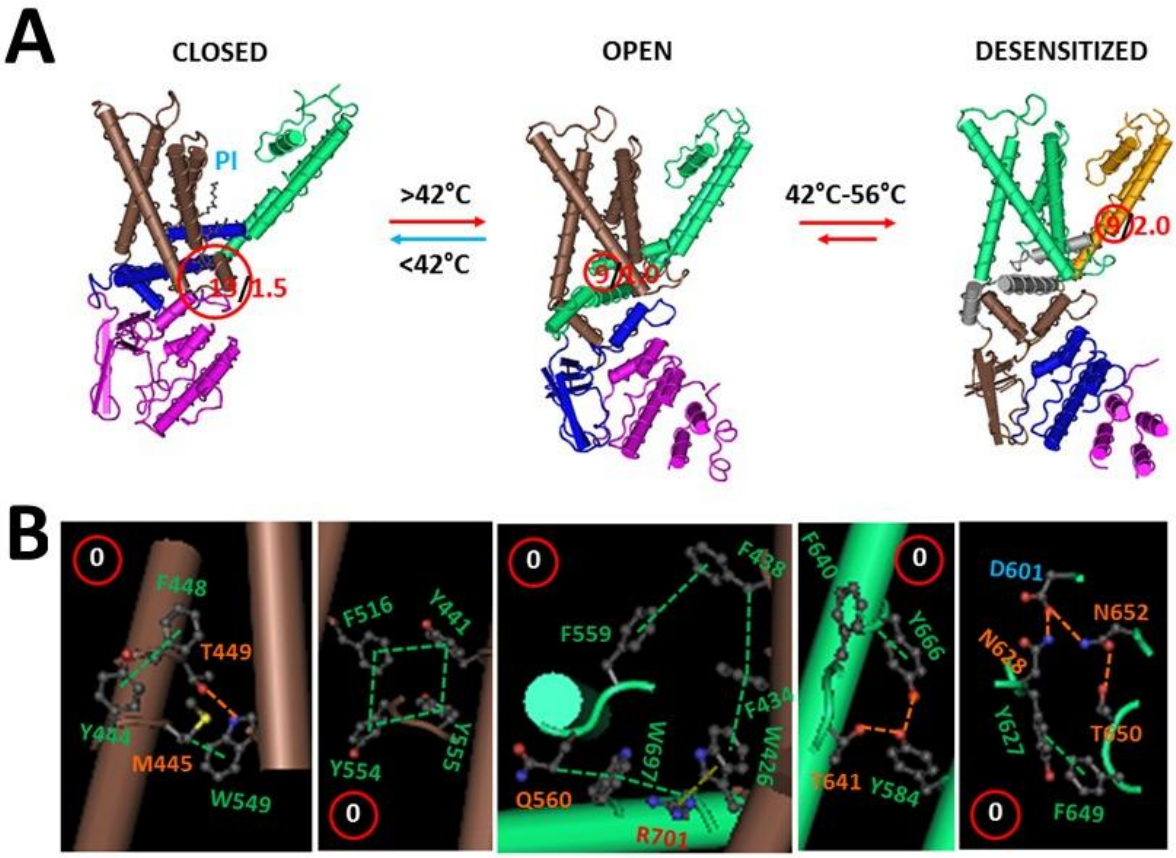
A
CLOSED
OPEN
DESENSITIZED
PI
>42°C
<42°C
42°C-56°C
1.5
2.0
B
F448
T449
Y444
M445
W549
F516
Y441
Y554
Y555
F559
F438
F434
W426
W697
Q560
R701
F640
Y666
T641
Y584
D601
N652
N628
Y627
T650
F649

Figure 5